

A mathematical model of cartilage regeneration after chondrocyte and stem cell implantation - II: The effects of co-implantation

Journal:	<i>Journal of Tissue Engineering</i>
Manuscript ID	JTE-Oct-18-0071.R1
Manuscript Type:	The Role and Contributions of Mathematical Modelling in Tissue Engineering and Regenerative Medicine
Date Submitted by the Author:	21-Dec-2018
Complete List of Authors:	Campbell, Kelly; Keele University, School of Computing and Mathematics Naire, Shailesh; Keele University, School of Computing and Mathematics Kuiper, Jan Herman; Keele University, Institute for Science and Technology in Medicine; Robert Jones and Agnes Hunt Orthopaedic Hospital NHS Foundation Trust
Keywords:	Mathematical Modelling, Co-culture, Mesenchymal Stem Cells, Cartilage Defect, Growth Factors
Abstract:	We present a mathematical model of cartilage regeneration after cell therapy, to show how co-implantation of stem cells (MSCs) and chondrocytes into a cartilage defect can impact chondral healing. The key mechanisms involved in the regeneration process are simulated by modelling cell proliferation, migration and differentiation, nutrient diffusion and ECM synthesis at the defect site, both spatially and temporally. In addition, we model the interaction between MSCs and chondrocytes by including growth factors. In Part I of this work, we have shown that matrix formation was enhanced at early times when MSC-to-chondrocyte interactions due to the effects of growth factors were considered. In this paper, we show that the additional effect of co-implanting MSCs and chondrocytes further enhances matrix production within the first year in comparison to implanting only chondrocytes or only MSCs. This could potentially reduce healing time allowing the patient to become mobile sooner after surgery.

SCHOLARONE™
Manuscripts

A mathematical model of cartilage regeneration after chondrocyte and stem cell implantation - II: The effects of co-implantation

Journal Title

XX(X):1-18

©The Author(s) 2018

Reprints and permission:

sagepub.co.uk/journalsPermissions.nav

DOI: 10.1177/ToBeAssigned

www.sagepub.com/

SAGE

Kelly Campbell¹, Shailesh Naire¹ and Jan Herman Kuiper^{2,3}

Abstract

We present a mathematical model of cartilage regeneration after cell therapy, to show how co-implantation of stem cells (MSCs) and chondrocytes into a cartilage defect can impact chondral healing. The key mechanisms involved in the regeneration process are simulated by modelling cell proliferation, migration and differentiation, nutrient diffusion and ECM synthesis at the defect site, both spatially and temporally. In addition, we model the interaction between mesenchymal stem cells and chondrocytes by including growth factors. In Part I of this work, we have shown that matrix formation was enhanced at early times when MSC-to-chondrocyte interactions due to the effects of growth factors were considered. In this paper, we show that the additional effect of co-implanting MSCs and chondrocytes further enhances matrix production within the first year in comparison to implanting only chondrocytes or only MSCs. This could potentially reduce healing time allowing the patient to become mobile sooner after surgery.

Keywords

Mathematical modelling, cartilage defect, regenerative medicine, co-culture, mesenchymal stem cells

Introduction

Autologous Chondrocyte Implantation (ACI) is the most commonly used cell-based therapy to treat chondral defects¹. The treatment comprises obtaining chondrocytes from a small harvest of healthy cartilage, a period of culturing the chondrocytes to expand their numbers, and implantation of these cells into the defect under a membrane. It does have some drawbacks, in particular the need for an extra knee surgery procedure to harvest the chondrocytes, difficulties in obtaining an adequate number of chondrocytes, and donor site morbidity². Mesenchymal stem cells (MSCs) are increasing in popularity as a cell source for regenerative medicine approaches for cartilage regeneration, such as cell implantation to treat articular cartilage defects of the joints³. The benefits of using MSCs instead of chondrocytes have been well documented, including their larger availability within the body and their ability to undergo chondrogenesis and deposit matrix under the influence of growth factors⁴.

An alternative cell-based therapy, denoted here as Articular Stem Cell Implantation (ASI), reproduces the approach of culture-expansion and implantation, except MSCs are used instead of chondrocytes². Lutianov *et al.*⁵

developed a mathematical model to simulate and compare the repair of a chondral defect with new cartilage following implantation of either chondrocytes (ACI) or MSCs (ASI) along the bottom of the defect. This model assumed that following implantation MSCs only contributed to cartilage formation via their differentiation into chondrocytes. One difference between ACI and ASI according to this model was that cartilage formation after ASI started later than after ACI. As is now widely recognised, MSCs used in this way do not only contribute to the repair process via their differentiation into chondrocytes but also via their secretion of growth factors and cytokines, termed as their "trophic" effect^{6,10}. Work by Wu *et al.*¹¹ identifies two growth factors, FGF-1 and BMP-2, as particularly

¹School of Computing and Mathematics, Keele University, Keele, ST5 5BG, U.K.

²Institute of Science and Technology in Medicine, Keele University, Keele, ST5 5BG, U.K.

³Robert Jones and Agnes Hunt Orthopaedic & District Hospital NHS Trust, Oswestry, SY10 7AG, U.K.

Corresponding author:

Kelly Campbell, School of Computing and Mathematics, Keele University, Keele, ST5 5BG, U.K.

Email: k.campbell@keele.ac.uk

important during cartilage regeneration. These two growth factors were identified when investigating the effect of co-cultures of MSCs and chondrocytes on cartilage formation¹¹. They are released by MSCs and chondrocytes and mediate MSC-to-chondrocyte interaction, enhancing chondrocyte proliferation and mesenchymal stem cell chondrogenesis (see Fig. 3 for a schematic of this cell-to-cell interaction in Part I of our work¹²). Their observations were modelled mathematically in Part I, which studied the effects of these growth factors after MSC implantation (ASI) into the defect¹². Our simulations showed that matrix formation following ASI was enhanced at early times when cell-to-cell interactions mediated by these growth factors were taken into account. This was mainly due to the presence of BMP-2, resulting in increased formation of chondrocytes **via increased chondrocyte proliferation and MSC chondrogenesis**, and hence enhancing early matrix production in comparison to the case when no growth factors are present. At later time points no differences were found.

Several *in vitro* studies have suggested that co-culturing a mixture of MSCs and chondrocytes increases matrix formation⁷⁻¹⁰. In these mixtures, the chondrocytes could immediately start forming cartilage and trophic effects due to the growth factors released in the system would boost this further¹¹. However, these *in vitro* studies are by necessity short-term studies and it is therefore not clear how these differences develop in the longer term and if they are maintained. To our knowledge, the only *in vivo* study used a rat model and found no difference in quality of cartilage defect repair 12 weeks after implanting scaffolds with either a 90:10 MSC:chondrocyte mixture or pure chondrocytes but did not study other time points¹³.

In Part II of our work, we aim to explore the longer term patterns over time of cartilage defect healing following implantation of mixtures of MSCs and chondrocytes at various ratios, and investigate the differences between them. The plan of the paper is as follows. In the section *Mathematical model*, we state the model equations, boundary and initial conditions. Next, *Results* shows the results of simulations for five co-implantation ratios and their comparison with respect to matrix density levels over healing time. Results showing sensitivity to variations in co-implantation ratios are also considered here, in particular, comparisons are made with 100% stem cells (ASI) and 100% chondrocytes (ACI) implantations. Finally, section *Discussion* explores the implications of the model results on co-culture cell therapy and future work. **We refer the interested reader to Campbell *et al.*¹² where full details**

of non-dimensionalisation and a sensitivity analysis of the model has been conducted, which will not be shown here.

Mathematical model

Our mathematical model follows the same formulation as our earlier work¹² with the initial cell implantation profile changed to accommodate a varying ratio of stem cells and chondrocytes. We only state the dimensionless equations, and boundary and initial conditions here. For more information on the formulation **and non-dimensionalisation** of these equations and assumptions made, the reader is referred to **Campbell *et al.*¹² and Lutianov *et al.*⁵**.

We consider a cartilage defect with a small depth to diameter ratio (see Fig. 1) which enables us to simplify to a one-dimensional problem where cell growth is modelled along the defect depth x only, with $x = 0$ at the base of the defect. The variables in our model are: the stem cell density C_S , the chondrocyte density C_C , the matrix density m , the nutrient concentration n , the FGF-1 concentration g and the BMP-2 concentration b . Cell density is measured in number of cells per unit volume, matrix density and growth factor concentration are measured as mass per unit volume and nutrient concentration is measured in number of moles per unit volume.

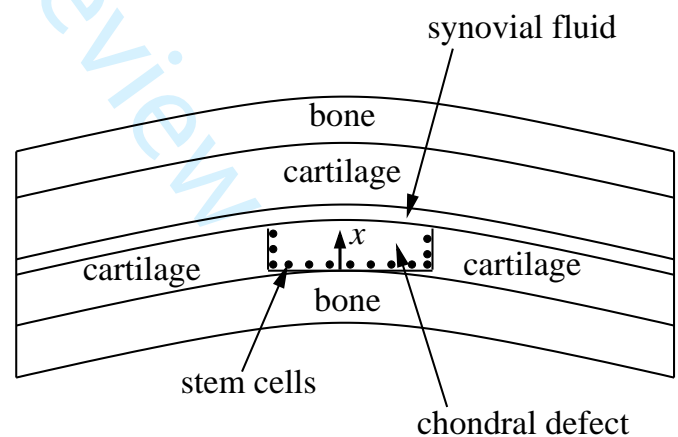


Figure 1. Schematic cross-section of a chondral defect. The thickness along the defect is labelled x .

Following the non-dimensionalisation given in **Campbell et al.**¹² and provided in the Appendix, the dimensionless equations (**overbars omitted**), boundary and initial conditions for the evolution of the cell and matrix densities and nutrient concentration in time, t , and space, x are given by:

$$\begin{aligned} \frac{\partial C_S}{\partial t} = & \frac{\partial}{\partial x} \left(D_S(m) \frac{\partial C_S}{\partial x} \right) \\ & + p_1 \left(m, \frac{C_S}{C_{S,max}(m)} \right) \frac{n}{n+n_0} C_S H(n-n_1) \\ & - p_2 C_S H(C_S - C_{S_0}(b)) - p_3 C_S H(n_1 - n), \quad (1a) \end{aligned}$$

$$\begin{aligned} \frac{\partial C_C}{\partial t} = & \frac{\partial}{\partial x} \left(D_C(m) \frac{\partial C_C}{\partial x} \right) \\ & + p_4 \left(m, g, \frac{C_C}{C_{C,max}(m)} \right) \frac{n}{n+n_0} C_C H(n-n_1) \\ & + p_2 C_S H(C_S - C_{S_0}(b)) - p_5 C_C H(n_1 - n), \quad (1b) \end{aligned}$$

$$\frac{\partial n}{\partial t} = D_n \frac{\partial^2 n}{\partial x^2} - \frac{n}{n+n_0} (p_6 C_S + p_7 C_C), \quad (1c)$$

$$\frac{\partial m}{\partial t} = D_m \frac{\partial^2 m}{\partial x^2} + p_8(m, g) \frac{n}{n+n_0} C_C, \quad (1d)$$

$$\frac{\partial g}{\partial t} = D_g \frac{\partial^2 g}{\partial x^2} + p_9 C_S - p_{11} g, \quad (1e)$$

$$\frac{\partial b}{\partial t} = D_b \frac{\partial^2 b}{\partial x^2} + p_{12} C_C - p_{13} b, \quad (1f)$$

where

$$\begin{aligned} p_1 \left(m, \frac{C_S}{C_{S,max}(m)} \right) &= A(m) \left(1 - \frac{C_S}{C_{S,max}(m)} \right), \\ A(m) &= p_{10} \frac{m}{m^2 + m_2^2}, \\ p_4 \left(m, g, \frac{C_C}{C_{C,max}(m)} \right) &= B(m) \left(1 - \frac{C_C}{C_{C,max}(m)} \right), \\ B(m) &= p_{40} \frac{m}{m^2 + m_2^2} + p_{400} \frac{g}{g+1}, \\ C_{S,max}(m) &= C_{S,max_0} (1 - m), \\ C_{C,max}(m) &= C_{C,max_0} (1 - m), \\ C_{S,max_0} + C_{C,max_0} &= 1, \\ p_8(m, g) &= (1 - p_{81} m) (1 + p_{800} \frac{g}{g+1}), \\ D_S(m) &= D_{S_0} \frac{m}{m^2 + m_1^2}, \quad D_C(m) = D_{C_0} \frac{m}{m^2 + m_1^2}, \\ C_{S_0}(b) &= (C_{S_0,max} - C_{S_0,min}) e^{-\alpha b} + C_{S_0,min}. \end{aligned} \quad (2)$$

The estimated values of the parameters in dimensional form and the dimensionless parameters are provided in the Appendix (Tables 1 and 2) and **Campbell et al.**¹².

The non-dimensional boundary and initial conditions are:

$$\begin{aligned} -D_S(m) \frac{\partial C_S}{\partial x} &= -D_C(m) \frac{\partial C_C}{\partial x} = -D_n \frac{\partial n}{\partial x} \\ &= -D_m \frac{\partial m}{\partial x} = -D_g \frac{\partial g}{\partial x} = -D_b \frac{\partial b}{\partial x} = 0, \quad (\text{at } x = 0), \end{aligned} \quad (3a)$$

$$\begin{aligned} -D_S(m) \frac{\partial C_S}{\partial x} &= -D_C(m) \frac{\partial C_C}{\partial x} = -D_m \frac{\partial m}{\partial x} = 0, \\ n = 1, \quad -D_g \frac{\partial g}{\partial x} &= \gamma g, \quad -D_b \frac{\partial b}{\partial x} = \chi b, \quad (\text{at } x = 1), \\ \mathbf{C}_S &= (1 - p_c) \mathbf{C}_S^{(0)} \mathbf{h}(\mathbf{x}), \quad \mathbf{C}_C = p_c \mathbf{C}_C^{(0)} \mathbf{h}(\mathbf{x}), \quad (3b) \\ n = 1, \quad m = m_3, \quad g &= g_{init}, \quad b = b_{init}, \quad (\text{at } t = 0). \end{aligned} \quad (3c)$$

with γ and χ representing the flux of growth factors leaving the top of the defect.

The new initial conditions representing the different co-culture ratios of stem cells and chondrocytes are highlighted in bold in Eq. (3). Here, $C_S^{(0)}$ and $C_C^{(0)}$ are the initial stem cell and chondrocyte densities, $h(x)$ is the initial profile and p_c ($0 \leq p_c \leq 1$) represents the proportion of chondrocytes implanted in the defect (e.g. a 35% chondrocyte proportion means $p_c = 0.35$, a mixture consisting of 65% stem cells and 35% chondrocytes at $t = 0$).

We used a second order accurate finite difference scheme to discretise the spatial derivatives in x **over 100 grid points** in Eqs. 1-3, keeping the time derivative t continuous. The resulting ordinary differential equations were solved in MATLAB (Release 2013a, The MathWorks Inc., Natick, Massachusetts, United States) using the stiff ODE solver *ode15s*. The dimensionless parameter values used in our simulations are **given in Table 2**.

The initial stem cell and chondrocyte density spatial profile is $C_S(x, 0) = C_S^{(0)} (1 - p_c) [1 - \tanh(A(x - x_0))]/2$ and $C_C(x, 0) = C_C^{(0)} p_c [1 - \tanh(A(x - x_0))]/2$, with $A = 10^4$ and $x_0 = 0.1$. Dimensionally, this is equivalent to a combined chondrocyte and stem cell density of 2.5×10^5 cells/mm³, restricted to an area of thickness $200 \mu\text{m}$ near $x = 0$, and zero elsewhere. We also assumed a small density of matrix ($m_3 = 10^{-4}$), FGF-1 ($g = g_{init}$) and BMP-2 ($b = b_{init}$) uniformly distributed across the defect.

The general evolution characteristics of the cell and matrix densities, nutrient and growth factor concentrations using this model are described in Part I of this work **Campbell et al.**¹² and in **Lutianov et al.**⁵ and hence are not repeated in detail here. The main focus of our simulations is to vary the initial stem cell and chondrocyte implantation densities through the parameter p_c , keeping the other parameters fixed.

1 We simulate cartilage repair following implantation of
2 **five mixtures**, namely $p_c = 0.1$ (90% stem cells and 10%
3 chondrocytes, hereafter referred to as 90:10), $p_c = 0.3$ (**70%**
4 **stem cells and 30% chondrocytes**, hereafter referred to
5 **as 70:30**), $p_c = 0.5$ (50% stem cells and 50% chondrocytes,
6 hereafter referred to as 50:50), $p_c = 0.7$ (**30% stem cells**
7 **and 70% chondrocytes**, hereafter referred to as **30:70**)
8 **and** $p_c = 0.9$ (**10% stem cells and 90% chondrocytes**,
9 hereafter referred to as **10:90**).
10
11
12
13
14
15
16
17
18
19
20
21
22
23
24
25
26
27
28
29
30
31
32
33
34
35
36
37
38
39
40
41
42
43
44
45
46
47
48
49
50
51
52
53
54
55
56
57
58
59
60

For Peer Review

Results

Co-implantation of 90% stem cells and 10% chondrocytes

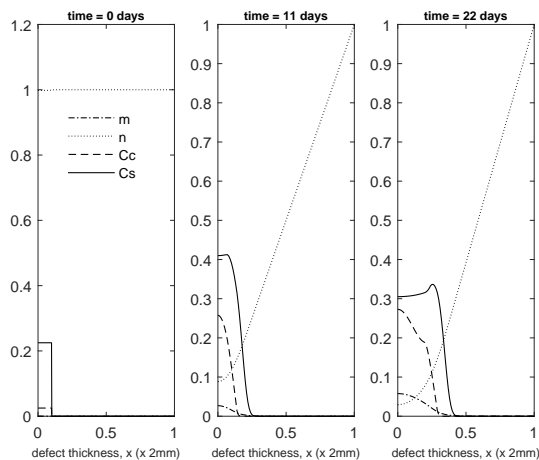


Figure 2. Evolution of cell and matrix densities, and nutrient concentration at times $t=0$, 11 and 22 days following co-implantation of 90% stem cells and 10% chondrocytes.

We first show the simulations corresponding to $p_c = 0.1$ (90% stem cells and 10% chondrocytes; 90:10). Panels 2 and 3 in Fig. 2 show the evolution at $t = 11$ and 22 days, respectively. Matrix production near $x = 0$ is seen after only a few days, mainly due to a rapid increase in chondrocyte density (almost 10 times the initial number within 11 days; see Panel 2 in Fig. 2). This early matrix production is of comparable magnitude to that produced for $p_c = 1.0$ (implantation of 100% chondrocytes; see Panel 2 in Fig. 2 of Lutianov *et al.*⁵), but using a far smaller number of chondrocytes (see Panel 2 in Fig. 2 of Lutianov *et al.*⁵) and occurs much earlier than for $p_c = 0$ (implantation of 100% stem cells), which requires 2 months to achieve similar matrix levels (Fig. 5 in Campbell *et al.*¹²). Over the course of the first few months, chondrocyte density is generally larger in the co-implantation case compared to the 100% stem cell and 100% chondrocyte implantation cases (compare Fig. 3 with Fig. 5 in Campbell *et al.*¹² and Fig. 3 in Lutianov *et al.*⁵). This larger chondrocyte density comes with increased matrix production but also with increased uptake of nutrients. The latter results in a drop of chondrocyte density towards the bottom of the defect once the nutrient concentration falls below the minimum threshold level $n_1 = 10^{-1}$, increasing chondrocyte death and slowing down chondrocyte proliferation. The net result is a slowing down of matrix production at the bottom of the defect. On the other hand, chondrocyte density continues to grow at the top of the defect due to the local abundance of nutrients there,

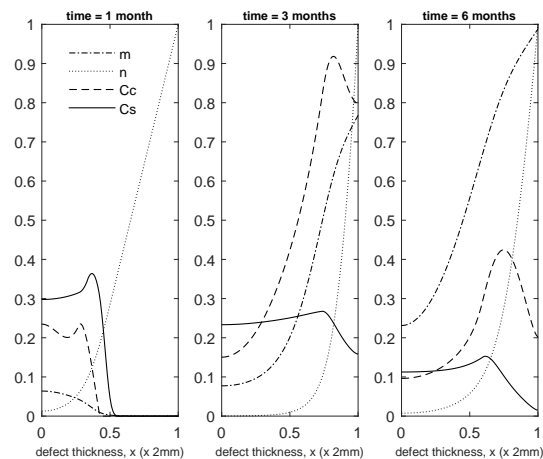


Figure 3. Evolution of cell and matrix densities, and nutrient concentration at times $t=1$, 3 and 6 months following co-implantation of 90% stem cells and 10% chondrocytes.

resulting in a continued increase in matrix density near the top of the defect (see Panels 2 and 3 in Fig. 3). At later times

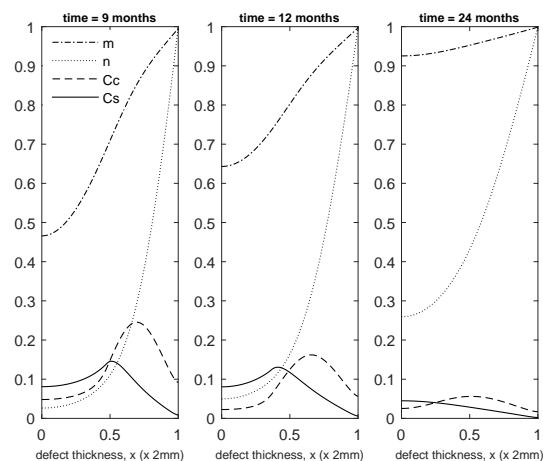


Figure 4. Evolution of cell and matrix densities, and nutrient concentration at times $t=9$, 12 and 24 months following co-implantation of 90% stem cells and 10% chondrocytes.

(Fig. 4), matrix deposition slows down and the defect fills up in 18-24 months. This time scale is similar to the two single cell type implantation cases (Fig. 4 in Lutianov *et al.*⁵ and Fig. 6 in Campbell *et al.*¹²).

Co-implantation of 70% stem cells and 30% chondrocytes

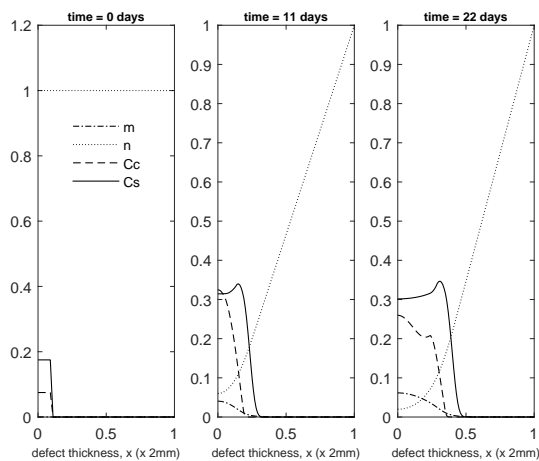


Figure 5. Evolution of cell and matrix densities, and nutrient concentration at times $t=0$, 11 and 22 days following co-implantation of 70% stem cells and 30% chondrocytes.

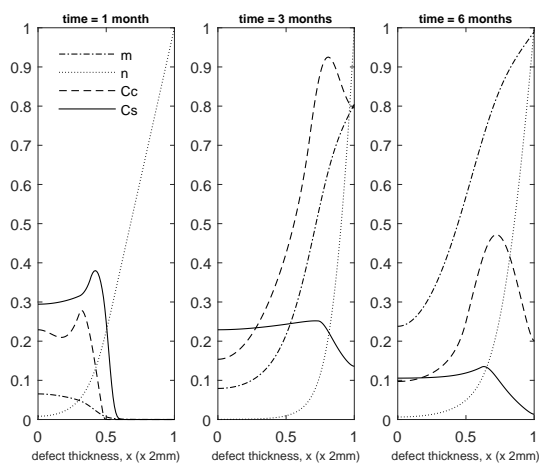


Figure 6. Evolution of cell and matrix densities, and nutrient concentration at times $t=1$, 3 and 6 months following co-implantation of 70% stem cells and 30% chondrocytes.

Next we show simulations of $p_c = 0.3$ corresponding to 70% stem cells 30% chondrocytes (70:30). Figures 5-7 show the evolution of the cell and matrix densities and nutrient concentration for time ranging between 11 days and 24 months. Similar to the 90:10 case (Figs. 2-4) we see enhanced matrix production at early time points with the nutrient concentration falling below the critical condition, $n_1 = 10^{-1}$, as early as 11 days at the bottom of the defect. This large consumption of nutrients is due to cell proliferation and MSC differentiation, which is enhanced due to FGF-1 and BMP-2^{11,12}. This decreases chondrocyte proliferation at the bottom of the defect, meaning diffusion of cells to higher concentrations

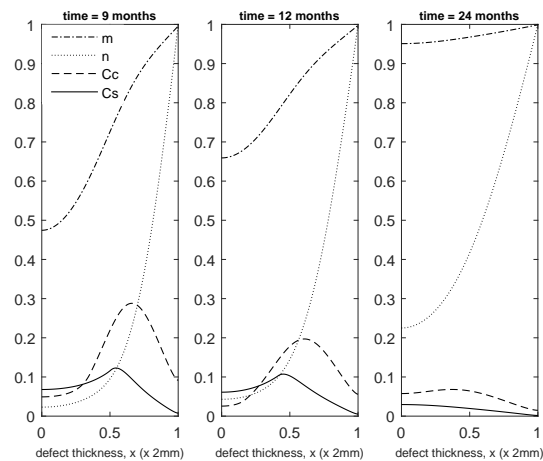


Figure 7. Evolution of cell and matrix densities, and nutrient concentration at times $t=9$, 12 and 24 months following co-implantation of 70% stem cells and 30% chondrocytes.

of nutrients will be the main driver of defect healing. As time continues, we see the general evolutionary characteristics of the simulations remain similar to our 90:10 case, albeit with slightly higher matrix levels due to the higher proportion of chondrocytes inserted into the defect. The defect is observed to fill-up with new cartilage within 18-24 months, which is in line with our previous results¹².

Co-implantation of 50% stem cells and 50% chondrocytes

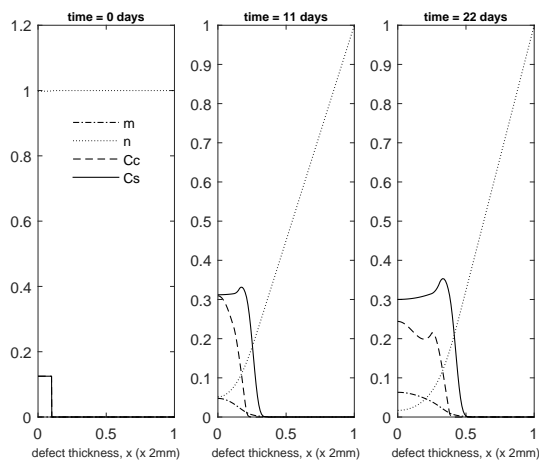


Figure 8. Evolution of cell and matrix densities, and nutrient concentration at times $t = 0, 11$ and 22 days following co-implantation of 50% stem cells and 50% chondrocytes.

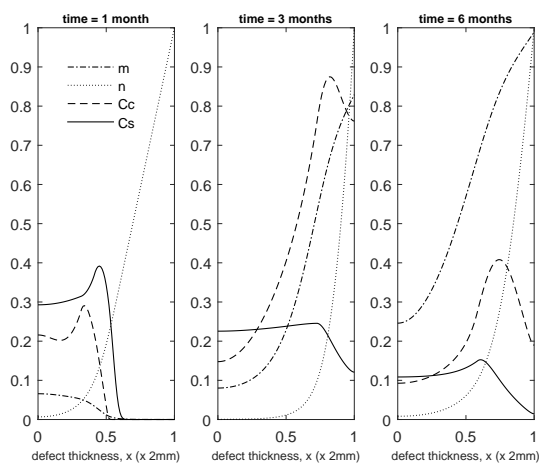


Figure 9. Evolution of cell and matrix densities, and nutrient concentration at times $t = 1, 3$ and 6 months following co-implantation of 50% stem cells and 50% chondrocytes.

We next show the simulations corresponding to $p_c = 0.5$ (50% stem cells and 50% chondrocytes; 50:50). Figures 8-10 show the evolution of the cell and matrix densities and nutrient concentration for this case at early and late time points. The evolution characteristics are identical to the 90:10 and 70:30 cases, except that the overall matrix density is slightly higher, particularly at earlier times (compare Panel 2 Fig. 8 and Fig. 2). This is a consequence of the larger proportion of implanted chondrocytes and the subsequent increase in chondrocyte density due to a combination of growth factor enhanced proliferation and stem cell differentiation. However, at later time points the increased nutrition demand from the larger overall cell density causes

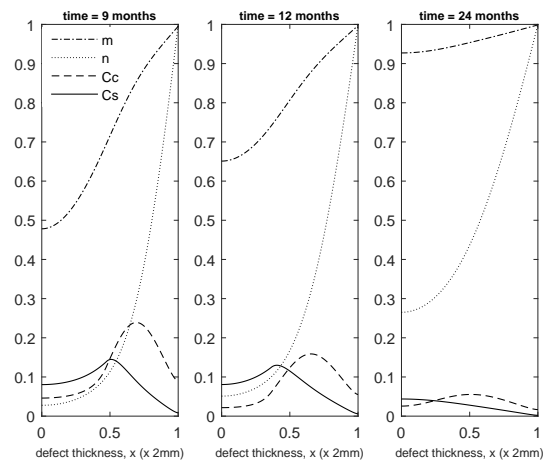


Figure 10. Evolution of cell and matrix densities, and nutrient concentration at times $t = 9, 12$ and 24 months following co-implantation of 50% stem cells and 50% chondrocytes.

the nutrient concentration close to the bottom of the defect to fall below the minimum threshold level $n_1 = 10^{-1}$, in turn slowing down cell proliferation and matrix production rates. Thus, the matrix density at later times is very similar to the 90:10 and 70:30 cases (compare Fig. 9 with Fig. 3 and Fig. 6).

Co-implantation of 30% stem cells and 70% chondrocytes

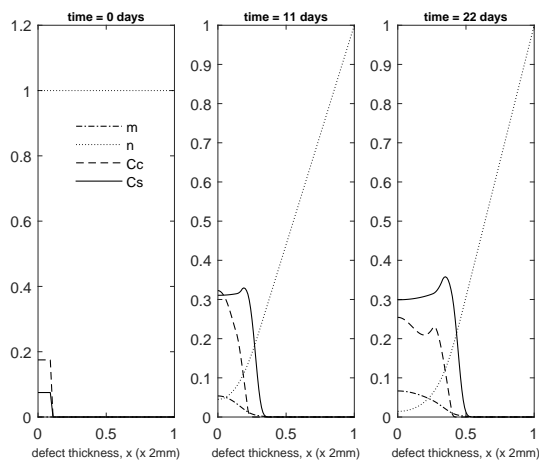


Figure 11. Evolution of cell and matrix densities, and nutrient concentration at times $t = 0, 11$ and 22 days following co-implantation of 30% stem cells and 70% chondrocytes.

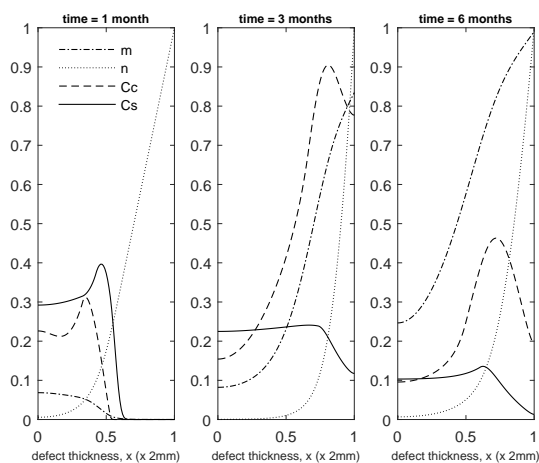


Figure 12. Evolution of cell and matrix densities, and nutrient concentration at times $t = 1, 3$ and 6 months following co-implantation of 30% stem cells and 70% chondrocytes.

Figures 11-13 show cell and matrix densities, and nutrient concentration for $p_c = 0.7$ simulations corresponding to 30% stem cells 70% chondrocytes (30:70). Here we observe high levels of matrix at early times. As with the other cases, nutrients are a limiting factor on healing, falling below the critical concentration and switching off cell proliferation by 11 days. MSCs appear to begin diffusing towards the top of the defect sooner in this case when compared with the 90:10 case (Fig. 2), for instance, likely to be due to higher matrix density allowing for cell motility. Once cell diffusion to the top of the defect has begun, we observe similar trends to the previous cases (Figs. 3, 6, 9). By 9 months (Fig. 13) matrix

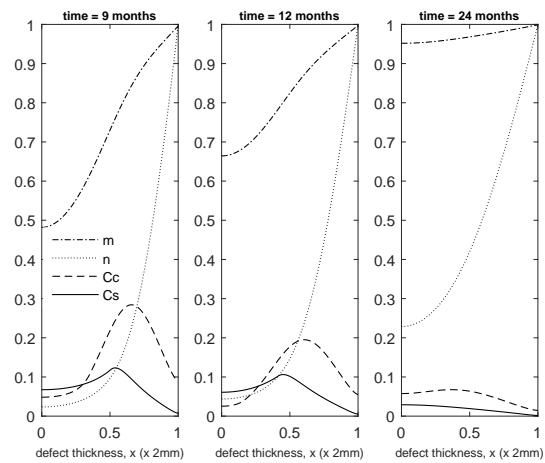


Figure 13. Evolution of cell and matrix densities, and nutrient concentration at times $t = 9, 12$ and 24 months following co-implantation of 30% stem cells and 70% chondrocytes.

densities are similar to those of our previous cases (Figs. 4, 7, 10), indicating the differences we see at early times are not maintained as time continues. This could be due to limited nutrient concentration, which is consistently low during the evolution.

Co-implantation of 10% stem cells and 90% chondrocytes

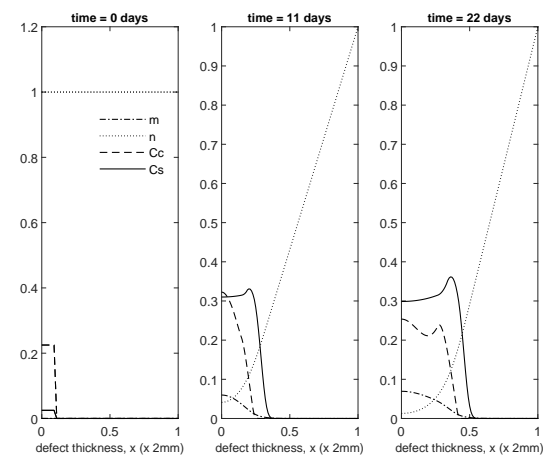


Figure 14. Evolution of cell and matrix densities, and nutrient concentration at times $t = 0, 11$ and 22 days following co-implantation of 10% stem cells and 90% chondrocytes.

We finally show the results for a 90% chondrocyte and 10% MSC mixture corresponding to $p_c = 0.9$ (10:90) (Figures 14, 15, 16). Here we have the highest proportion of chondrocytes inserted into the defect, and as such have the highest matrix levels at early times. This is likely due to increased matrix formation primarily occurring at early times during our simulations, when nutrients are

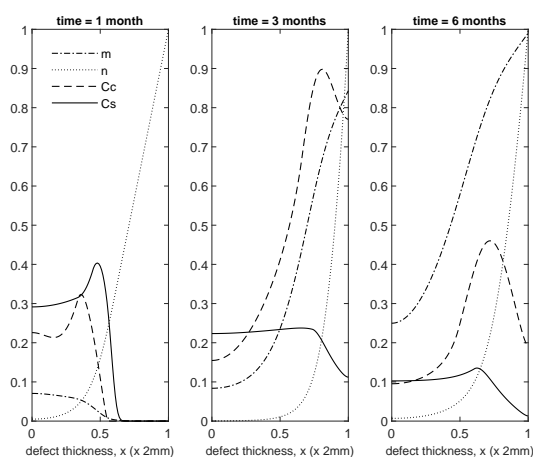


Figure 15. Evolution of cell and matrix densities, and nutrient concentration at times $t = 1, 3$ and 6 months following co-implantation of 10% stem cells and 90% chondrocytes.

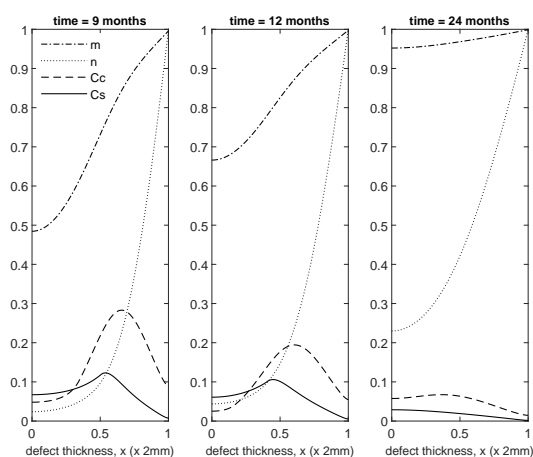


Figure 16. Evolution of cell and matrix densities, and nutrient concentration at times $t = 9, 12$ and 24 months following co-implantation of 10% stem cells and 90% chondrocytes.

more readily available in the defect. This means a higher implanted chondrocyte density, as demonstrated here, could be desirable to increase matrix levels. Despite this, as with our previous co-implantation cases, increased matrix deposition appears to slow at later times, with nutrient concentration and cell diffusion being the main regulatory factors of healing.

Next, we make a comparison between the five co-implantation cases with ACI and ASI to identify both spatial and temporal differences in matrix and cell densities.

Comparison of matrix density of co-implantation, ACI and ASI at early times

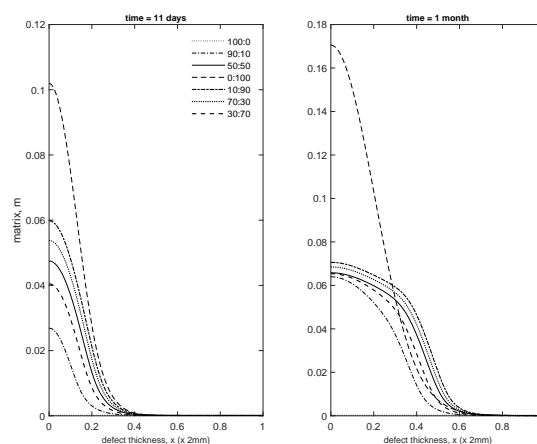


Figure 17. Comparison of matrix density profiles for all cases at times $t = 11$ days and 1 month.

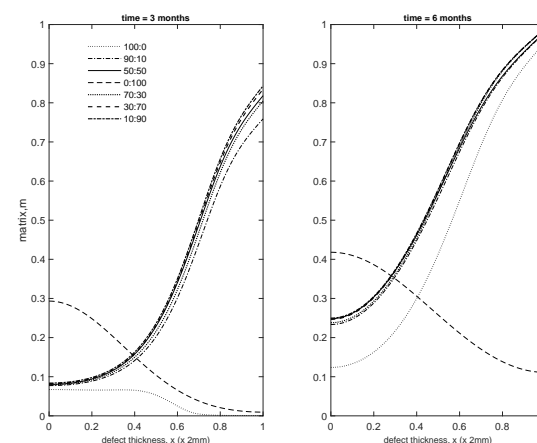


Figure 18. Comparison of matrix density profiles for all cases at times $t = 3$ and 6 months.

Figures 17 and 18 compare matrix densities at early times for five co-implantation cases with ACI and ASI.

Up to 1 month, the 100% chondrocyte case (0:100) has the largest amount of matrix (Fig. 17). Although at 11 days the chondrocyte density in the 90:10 case is close to that of other co-implantation cases containing higher chondrocyte densities, and even higher than in the 0:100 case (compare Figs. 2, 5, 8, 11, 14 and Fig 2 in Lutianov et al.⁵), the additional nutrient demands of the stem cells brings the nutrient concentration below the minimum threshold value, resulting in matrix densities much lower

than the 0:100 case (Fig. 17). In the 100:0 case, the stem cells have not yet differentiated into chondrocytes at these early time points and hence no matrix at all is produced (Fig. 17).

The 10:90 case has the highest levels of matrix at 3 months (Panel 1 in Fig. 18), consistent with the observations in Figures 14, 15, 16. The five co-implantation cases produce more matrix than the 0:100 case, despite the 0:100 case having the largest matrix density at earlier times and the highest implantation of chondrocytes. The 100:0 implantation, relevant to ASI, still has the lowest matrix levels, indicating that the implantation of mesenchymal stem cells alone delays healing initially (Panel 1 in Fig. 18).

These findings highlight the importance of early matrix deposition, as it is clear at late times the differences we observe in matrix levels between our co-implantation cases are more moderate (Figs. 4, 7, 10, 13, 16, Panel 2 in 18). At late times our simulations are more likely to be constrained by low nutrient concentrations, therefore slowing the rate of healing down. At early times more nutrients are available within the defect, primarily at the top, where formation of cartilage is most notable in our ASI and co-implantation cases. We find our ACI case forms matrix primarily at the bottom of the defect as nutrient levels never become very low here, unlike for our other cases, meaning cells are not forced to diffuse to areas of higher nutrient concentration to continue proliferating (Fig. 18). Chondrocytes also have a lower cell motility rate in comparison to MSCs, meaning diffusion to the top of the defect will be slower.

Comparing mean cell and matrix densities versus time for co-implantation, ACI and ASI

Here we compare the mean matrix, chondrocyte and MSC densities over a period of 24 months for 4 cases: 0:100 (ACI), 100:0 (ASI), and 2 co-implantation strategies, 90:10 and 10:90. We choose to focus on 90:10 and 10:90 as they represent our two most extreme co-implantation cases, with all other results, i.e. 70:30, 50:50 and 30:70, lying within the bounds of these two sets of results (see Figs. 17 and 18). The two single-cell implantation cases are investigated in Lutianov *et al.*⁵ and Part I of our work Campbell *et al.*¹², and the interested reader is referred to these studies.

In Figure. 19(a), at 1 month, the mean matrix density produced is largest for the 0:100 case (blue). This is

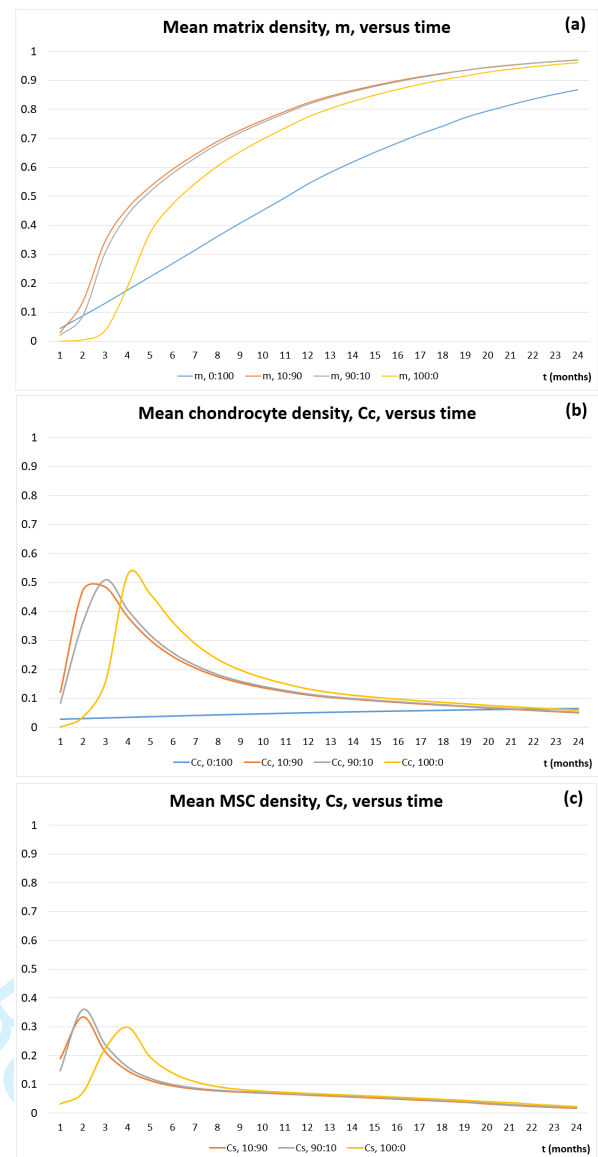


Figure 19. Mean densities of (a) matrix, m , (b) chondrocytes, C_C , (c) MSCs, C_S , as a function of the time, in months, from 1-24 months for 0:100 (ACI, blue), 10:90 (orange), 90:10 (grey) and 100:0 (ASI, yellow).

not only because this case has the largest concentration of chondrocytes directly producing matrix from the beginning, but also because only chondrocytes are seeded in the defect. The co-implantation cases also have a population of stem cells competing for nutrients, thus reducing the average matrix production by the chondrocytes. At 2 months the 100:0 (grey) case has produced barely any matrix due to MSCs having to first differentiate into chondrocytes before matrix deposition can begin. Also at this time, our co-implantation cases (90:10 grey, 10:90 orange) have already surpassed the matrix levels of 0:100 despite containing less implanted chondrocytes. This is due to growth factors being released by the cell-to-cell interaction of the MSCs and

chondrocytes (Campbell *et al.*¹²) and the balance of the effects of cell proliferation and nutrient levels. In our model MSCs have a high demand for nutrients to support their high proliferation rate and their differentiation into chondrocytes. In the 90:10 case the large concentration of MSCs therefore consume a large amount of nutrients, leaving less for the chondrocytes to produce matrix. On the other hand, in the 10:90 case the MSC density is lower and therefore these cells consume less nutrients, leaving more nutrients for the chondrocytes to proliferate and deposit matrix. This difference is mainly observable at early times.

At 3 months the mean matrix density for 90:10 (grey) case 136% more than in the 0:100 case (blue), and an even higher percentage difference when compared with the 100:0 case (yellow). This marked increase in matrix density is due the effects of the growth factors¹². We see a higher percentage difference when compared to 100:0 due to lower mean chondrocyte density at this time compared to 90:10 and 0:100 (see Fig. 19(b) for the mean chondrocyte density comparison between the co-implantation cases and ACI and ASI). Beyond 3 months this increase in mean matrix levels is sustained for the co-implantation cases with an 80% increase at 12 months when compared with 0:100 for our 90:10 case. The percentage difference is smaller when compared with the 100:0 case, with a 5.5% increase at 12 months. Past 1 year we see the co-implantation cases maintain the highest mean matrix levels, which is an accumulation of the differences in matrix levels at early times.

In Fig. 19(b) we compare the mean chondrocyte densities for the 10:90 (orange), 90:10 (grey) and 100:0 (yellow) cases. We do not show the evolution of the mean cell density of the 0:100 case since it is more localised to the bottom of the defect and therefore not a good comparison for mean cell levels. We see at 1 month that the 10:90 case (orange) has the highest levels of chondrocytes, but despite this matrix deposition is slow initially due to nutrient levels falling below the critical condition, $n_1 = 10^{-1}$ (Fig. 9). This effect is also observable in the 90:10 case (orange). At 3 months chondrocyte levels have increased dramatically in our co-implantation cases, indicating MSC differentiation has been initiated, thus leading to these cases having the highest matrix density (Fig 19(a)).

In Fig. 19(c) we compare the mean MSC densities for the 10:90 (grey) and 90:10 (orange) co-implantation

and 100:0 (yellow) cases. The 0:100 contains no MSCs. At 1 month the 90:10 case has the highest density of MSCs, despite the 100:0 case having the highest implantation of MSCs. In the 10:90 and 90:10 cases cell-to-cell interaction releases growth factors almost immediately, meaning chondrocyte proliferation and MSC differentiation is enhanced^{11,12}. This is likely to be the cause of the marked increase in MSC levels in the defect at this time.

Discussion

This study aimed to develop a mathematical model to explore the longer term patterns over time of cartilage defect healing following implantation of mixtures of MSCs and chondrocytes at various ratio's, and investigate the differences between them. Firstly, our simulations suggest that co-implanting MSCs and chondrocytes will increase matrix deposition within the first half year of healing when compared with 100% mesenchymal stem cell (ASI) or 100% chondrocyte (ACI) implantation therapies, indicating a chondral defect could fill with new cartilage at earlier times when a co-culture procedure is the chosen treatment. Although 10:90 appears to have the highest matrix density at early times, clinically a co-implantation ratio that uses less chondrocytes is desirable if the aim would be to develop a single-stage autologous chondrocyte implantation procedure⁸. Opting for the lower proportion of chondrocytes in these co-implantation therapies could mean sufficient chondrocytes can be isolated from the cartilage harvest obtained during arthroscopy for a successful co-implantation procedure¹⁴. This alleviates the need for expansion of cells *in vitro* if the fresh chondrocytes are combined with allogeneic stem cells, allowing cells to be harvested and inserted into the defect region during one procedure¹⁵. Alternatively, the fresh chondrocytes can be mixed with fresh bone marrow, which despite the lower total cell number has been suggested to be clinically effective¹⁶.

Our model enabled us to compare matrix densities following co-implantation of MSCs and chondrocytes at various ratios, visualising not only the cartilage matrix density distribution at any time point, but also investigating how the concentrations of MSCs, chondrocytes and nutrients change within the defect in response to different co-implantation ratios. The five ratios we focused on were 90% MSCs plus 10% chondrocytes, 70% MSCs plus 30% chondrocytes, 50% MSCs plus 50% chondrocytes, 30% MSCs plus 70% chondrocytes and 10% MSCs plus 90% chondrocytes, with 90:10 and 50:50 having been

1
2 **or are being investigated clinically** ^{15,17}. **We compared**
3 **these to autologous chondrocyte implantation (ACI,**
4 **100% chondrocytes) and articular stem cell implantation**
5 **(ASI, 100% MSCs). When comparing co-implantation**
6 **scenarios with the ACI and ASI results from our**
7 **previous work** ^{5,12}, **it is clear that a mixture of MSCs**
8 **and chondrocytes delivers the desired effect of increased**
9 **matrix deposition, as hypothesised in the literature** ¹⁸ **and**
10 **in previous experiments** ¹¹. This effect is especially marked
11 during the first few months following cell implantation, but
12 from around six month onwards the differences, especially
13 with ASI, become small. As time progresses, the 0:100 case
14 continues to produce matrix at a steady rate, but the 100:0
15 and co-implantation cases soon surpass these levels. Figure
16 **19(a)** shows how total matrix levels of 100:0 (ASI), 90:10,
17 10:90 and 0:100 (ACI) simulations compare at over a period
18 of 2 years. At early time there is a monotonic increase
19 in the total matrix density with the 0:100 case having the
20 highest density, 100:0 having produced almost no matrix
21 at all, and the coimplantation cases having almost similar
22 intermediate levels of matrix. This indicates that at early time
23 chondrocyte proliferation balanced with adequate nutrient
24 availability is the main identifiable mechanism responsible
25 for the formation of new cartilage in our model. As time
26 progresses, 0:100 continues to produce matrix at a steady
27 rate, but 100:0 and co-implantation cases soon surpass these
28 levels. Beyond 6 months there is a non-monotonic increase
29 in the total matrix density with a peak in matrix levels in
30 the co-implantation cases, and the 100:0 case still producing
31 the lowest level of matrix. Although we cannot say with
32 any certainty that the maximum matrix density is obtained
33 precisely for the 10:90 or 90:10 case, there is a definite
34 optimal ratio of stem cells and chondrocytes that can produce
35 maximum matrix at intermediate times. This indicates that
36 at these times cell differentiation and diffusion are the
37 important mechanisms driving new cartilage formation.
38 From six months onwards, we found little difference in the
39 distribution of cell types and cartilage matrix between the
40 five co-implantation cases and implanting only stem cells.
41 This suggests that implanting a cell population that includes
42 stem cells will lead to a stable solution path, regardless of
43 the exact proportion of stem cells. Although co-implantation
44 of chondrocytes and stem cells led to more matrix deposition
45 at earlier time points, this difference was not maintained and
46 by 12 months the difference in matrix production between
47 the five cases was very small. Similar small differences
48 have been found between 1-year biopsies obtained in human
49 trials of co-implanted cells, stem cells or chondrocytes ^{2,15}.
50 Nevertheless, the larger matrix deposition at earlier time

may give advantages with respect to the rehabilitation, which
could be faster if matrix is formed earlier. This alone could
be an important clinical advance in the treatment of articular
cartilage damage.

A mixture of stem cells and chondrocytes produces
more consistent levels of matrix due to the balance of
nutrient used between the two cell types and the release
of important growth factors that influence chondrocyte
proliferation and stem cell differentiation. In our model, this
effect is partly due to the cell-cell interactions between MSCs
and chondrocytes, releasing growth factors such as FGF-
1 and BMP-2 that cause an increase in matrix deposition
from increased chondrocyte proliferation and enhanced
chondrogenesis (see also **Wu et al.** ¹¹). Additionally, the
increase of matrix deposition and chondrocyte density at
early times for our co-implantation cases is in part due to the
lower proliferation rate of the chondrocytes, allowing more
nutrients to be available in the defect for MSC proliferation
and differentiation.

An important assumption in our model concerns the
role of chondrogenesis, the differentiation of stem cells
into chondrocytes. Our results suggest that stem cell
differentiation played an important part in increasing the
number of chondrocytes, and eventually the matrix, due to
large quantities of chondrocytes, comparable to our 50:50
case, being present in the defect when 90% MSCs are
implanted. Most *in vitro* co-culture studies suggest that the
more important contribution from the stem cells is their
positive effect on chondrocyte proliferation whereas their
differentiation into chondrocytes is less important ¹⁰.

Other mixtures of MSCs and chondrocytes could be
investigated to find an 'optimal' MSC/chondrocyte ratio,
where nutrient constraints are minimised and matrix
deposition maximised. Our criterion for suggesting an
optimal co-implantation ratio is based on mean matrix
densities. However, other criteria could also be used
to determine an optimal ratio. Some justification of
our current criterion are clinical data comparing MRI
imaging and clinical outcome that suggests the signal
intensity on MRI correlates with better clinical outcome
of ACI (McCarthy et al. ²⁴). The signal intensity is a
measure of mean matrix density, and thus our chosen
measure will give a clinically relevant comparison.
However, other parameters such as the required time for
cartilage matrix to fill the defect and the required time
to achieve a threshold density at the surface might also
be appropriate. The spatial distribution of matrix might
also be relevant, as seen in Figs 17 and 18. However, our
results suggest that this may be difficult to translate in

1
2
3
4
5
6
7
8
9
10
11
12
13
14
15
16
17
18
19
20
21
22
23
24
25
26
27
28
29
30
31
32
33
34
35
36
37
38
39
40
41
42
43
44
45
46
47
48
49
50
51
52
53
54
55
56
57
58
59
60

a criterion. The comparison between MRI and clinical outcome suggests that the articular surface of the repair tissue may be most important²⁴, which would suggest that the repairs including stem cells, which form denser matrix at the defect surface, might be better. However, the distribution of matrix density is less homogeneous for these cases, and poor matrix homogeneity is associated with poorer clinical outcome²⁴. The limitations of our model dictate that all simulations are subject to nutrient concentration constraints, typically meaning an optimal split of MSCs and chondrocytes is not at all obvious; this would require further investigation. This effect of nutrient concentration impacting the overall healing process has been hypothesised in our previous model as well as similar work¹⁹, with this co-implantation model now corroborating this hypothesis further. Availability of cell types, overall cost and efficacy of the procedure are factors that would also have to be considered when considering an optimal MSC-chondrocyte co-implantation ratio.

Declaration of conflicting interests

The Authors declare that there is no conflict of interest.

Funding

We would like to acknowledge Keele University for funding this work which forms a part of Kelly Campbell's PhD research.

References

1. Mollon B, Kandel R, Chahal J et al. The clinical status of cartilage tissue regeneration in humans. *Osteoarthritis and cartilage* 2013; 21(12): 1824–1833.
2. Nejadnik H, Hui JH, Feng Choong EP et al. Autologous bone marrow-derived mesenchymal stem cells versus autologous chondrocyte implantation: an observational cohort study. *The American journal of sports medicine* 2010; 38(6): 1110–1116.
3. Filardo G, Perdisa F, Roffi A et al. Stem cells in articular cartilage regeneration. *Journal of orthopaedic surgery and research* 2016; 11(1): 42.
4. Roberts S, Genever P, McCaskie A et al. Prospects of stem cell therapy in osteoarthritis. *Regenerative medicine* 2011; 6(3): 351–366.
5. Lutianov M, Naire S, Roberts S et al. A mathematical model of cartilage regeneration after cell therapy. *Journal of Theoretical Biology* 2011; 289: 136–150.
6. Caplan AI and Dennis JE. Mesenchymal stem cells as trophic mediators. *Journal of cellular biochemistry* 2006; 98(5): 1076–1084.
7. Liu X, Sun H, Yan D, Zhang L, Lv X, Liu T, Zhang W, Liu W, Cao Y, Zhou G. In vivo ectopic chondrogenesis of BMSCs directed by mature chondrocytes. *Biomaterials* 2010; 31(36): 9406–9414.
8. Bekkers JEJ, Tsuchida AI, van Rijen MHP et al. Single-Stage Cell-Based Cartilage Regeneration Using a Combination of Chondrons and Mesenchymal Stromal Cells: Comparison With Microfracture. *The American Journal of Sports Medicine* 2013; 41(9): 2158–2166.
9. de Windt TS, Hendriks JAA, Zhao X et al. Concise Review: Unraveling Stem Cell Cocultures in Regenerative Medicine: Which Cell Interactions Steer Cartilage Regeneration and How? *Stem Cells Translational Medicine* 2014; 3(6): 723–733.
10. de Windt TS, Hendriks JA, Zhao X et al. Concise review: unraveling stem cell cocultures in regenerative medicine: which cell interactions steer cartilage regeneration and how? *Stem cells translational medicine* 2014; 3(6): 723–733.
11. Wu L. *Mesenchymal stem cells as trophic mediators in cartilage regeneration*. PhD Thesis, 2013.
12. Campbell K, Naire S and Kuiper JH. A mathematical model of cartilage regeneration after cell therapy mediated by growth factors : Part 1. *Journal of Tissue Engineering* 2018; : 0–1.
13. Dahlin RL, Kinard LA, Lam J et al. Articular chondrocytes and mesenchymal stem cells seeded on biodegradable scaffolds for the repair of cartilage in a rat osteochondral defect model. *Biomaterials* 2014; 35(26): 7460–7469.
14. Vonk LA, De Windt TS, Slaper-Cortenbach IC et al. Autologous, allogeneic, induced pluripotent stem cell or a combination stem cell therapy? where are we headed in cartilage repair and why: a concise review. *Stem cell research & therapy* 2015; 6(1): 94.
15. de Windt TS, Vonk LA, Slaper-Cortenbach IC et al. Allogeneic mscs and recycled autologous chondrons mixed in a one-stage cartilage cell transplantation: a first-in-man trial in 35 patients. *Stem cells* 2017; 35(8): 1984–1993.
16. Slynarski K, Widuchowski W, Snow M et al. Primary chondrocytes and bone marrow cells on a 3d co-polymer scaffold: 2-year results of a prospective, multicenter, single-arm clinical trial in patients with cartilage defects of the knee. *Revue de Chirurgie Orthopédique et Traumatologique* 2015; 101(8): e17–e18.
17. Richardson JB, Wright KT, Wales J et al. Efficacy and safety of autologous cell therapies for knee cartilage defects (autologous stem cells, chondrocytes or the two): randomized controlled trial design. *Regenerative medicine* 2017; 12(5): 493–501.
18. Hendriks J, Riesle J and van Blitterswijk CA. Co-culture in cartilage tissue engineering. *Journal of tissue engineering and regenerative medicine* 2007; 1(3): 170–178.

19. Zhou S, Cui Z and Urban JP. Nutrient gradients in engineered cartilage: metabolic kinetics measurement and mass transfer modeling. *Biotechnology and bioengineering* 2008; 101(2): 408–421.
20. Obradovic B, Meldon JH, Freed LE et al. Glycosaminoglycan deposition in engineered cartilage: experiments and mathematical model. *AIChE Journal* 2000; 46(9): 1860–1871.
21. Zhou S, Cui Z and Urban JP. Factors influencing the oxygen concentration gradient from the synovial surface of articular cartilage to the cartilage–bone interface: a modeling study. *Arthritis & Rheumatism* 2004; 50(12): 3915–3924.
22. Bailón-Plaza A and Vander Meulen MC. A Mathematical Framework to Study the Effects of Growth Factor Influences on Fracture Healing. *Journal of Theoretical Biology* 2001; 212(2): 191–209.
23. Zhang L, Hu J, Athanasiou K, The role of tissue engineering in articular cartilage repair and regeneration. *Critical reviews in biomedical engineering* 2009; 37(1-2): 1–57
24. McCarthy H, McCall I, Williams J, Mennan C, Dugard M, Richardson J, Roberts S, Magnetic Resonance Imaging Parameters at 1 Year Correlate With Clinical Outcomes Up to 17 Years After Autologous Chondrocyte Implantation. *Orthopaedic Journal of Sports Medicine* 2018; 6(8):1-10

Appendix: Non-dimensionalisation and estimates of dimensional and dimensionless parameters

The estimated values of the dimensional parameters appearing in the model and the references from which they are obtained are provided in Table 1.

dimensional parameters	estimated value
defect thickness, d	2-3 mm
maximum stem cell migration (or diffusion) coefficient, D_S	$3.6 \times (10^{-4} - 10^{-3}) \text{ mm}^2/\text{hr}$ 20
maximum chondrocyte migration (or diffusion), constant, D_C	$3.6 \times 10^{-4} \text{ mm}^2/\text{hr}$ 20
stem cell migration (or diffusion), constant, $D_{S_0} = 2m_1 D_S$	$7.2 \times (10^{-9} - 10^{-8}) (\text{mm}^2/\text{hr}) (\text{g}/\text{mm}^3)$ (assuming $m_1 = 10^{-5} \text{ g}/\text{mm}^3$)
chondrocyte migration (or diffusion), constant, $D_{C_0} = 2m_1 D_C$	$7.2 \times 10^{-9} (\text{mm}^2/\text{hr}) (\text{g}/\text{mm}^3)$ (assuming $m_1 = 10^{-5} \text{ g}/\text{mm}^3$)
nutrient diffusion coefficient, D_n	$4.6 \text{ mm}^2/\text{hr}$ ²¹
matrix diffusion coefficient, D_m	$2.5 \times 10^{-5} \text{ mm}^2/\text{hr}$ 20
FGF-1 diffusion coefficient, D_g	$2 \times 10^{-3} \text{ mm}^2/\text{hr}$ 22
BMP-2 diffusion coefficient, D_b	$2 \times 10^{-3} \text{ mm}^2/\text{hr}$ 22
maximum stem cell proliferation rate, p_1	0.2 cell/hr or 5 cells/day 22
stem cell proliferation constant, $p_{1_0} = 2m_2 p_1$	$4 \times 10^{-6} \text{ g}/\text{mm}^3/\text{hr}$ (assuming $m_2 = 10^{-5} \text{ g}/\text{mm}^3$)
stem cell differentiation rate, p_2	$3.75 \times 10^{-3}/\text{hr}$ 20
stem cell death rate, p_3	$3.75 \times 10^{-3}/\text{hr}$ (guess)
maximum chondrocyte proliferation rate, p_4	$2 \times 10^{-4}/\text{hr}$ (guess)
chondrocyte proliferation constant, $p_{4_0} = 2m_2 p_4$	$4 \times 10^{-9} \text{ g}/\text{mm}^3/\text{hr}$
chondrocyte death rate, p_5	$3.75 \times 10^{-3}/\text{hr}$ (guess)
FGF-1 production constant, p_9	$10^{-17} (\text{g}/\text{mm}^3)/((\text{Nc}/\text{mm}^3) \text{ hr})$ (guess)
BMP-2 production constant, p_{12}	$10^{-17} (\text{g}/\text{mm}^3)/((\text{Nc}/\text{mm}^3) \text{ hr})$ (guess)
FGF-1 degradation rate, p_{11}	$5.8 \times 10^{-2} /\text{hr}$ (based on 12hr half-life guess)
BMP-2 degradation rate, p_{13}	$5.8 \times 10^{-2} /\text{hr}$ (based on 12hr half-life guess)
chondrocyte proliferation rate (from FGF-1), p_{4_0}	$2 \times 10^{-4} /\text{hr}$ (guess)
matrix production constant, p_{8_0}	$3.75 \times 10^{-13} (\text{g}/\text{mm}^3)/((\text{Nc}/\text{mm}^3) \text{ hr})$ 20
matrix degradation constant, p_{8_1}	$3.75 \times 10^{-13} (\text{g}/\text{mm}^3)/((\text{Nc}/\text{mm}^3) \text{ hr})$ 20
nutrient uptake constant by stem cells, p_6	$1.5 \times 10^{-14} \text{ Nm}/(\text{Nc hr})$ 21
nutrient uptake constant by chondrocytes, p_7	$1.5 \times 10^{-14} \text{ Nm}/(\text{Nc hr})$ 21
FGF-1 matrix deposition rate, p_{8_0}	0 - 1 (guess)
maximum total cell density, C_{total,max_0}	$10^6 \text{ Nc}/\text{mm}^3$ (assuming $10 \mu\text{m}$ cell diameter)
maximum stem cell density, C_{S,max_0}	0 - $10^6 \text{ Nc}/\text{mm}^3$
maximum chondrocyte density, C_{C,max_0}	0 - $10^6 \text{ Nc}/\text{mm}^3$

maximum matrix density, m_{max}	10^{-4} g/mm ³ 22
initial stem cell density, $C_S^{(0)}$	2.5×10^5 Nc/mm ³ (based on 10^6 cells in 20mm x 20mm x 10 μ m volume)
initial cartilage cell density, $C_C^{(0)}$	10^2 Nc/mm ³ ($10^{-2}\%$ of total cell density)
threshold stem cell density, C_{S0max}	$C_{total,max0}/2$ Nc/mm ³ (guess)
threshold stem cell density, C_{S0min}	90% of C_{S0max} (guess)
matrix density, m_1	10^{-5} g/mm ³ (assumed $m_{max}/10$)
matrix density, m_2	10^{-5} g/mm ³ (assumed $m_{max}/10$)
initial matrix density, m_3	10^{-8} g/mm ³ (assumed $m_{max}/10^4$)
initial nutrient concentration, N_0	$(2.85 - 9.5) \times 10^{-11}$ Nm/mm ³ 21
initial FGF-1 concentration, g_{init}	10^{-12} g/mm ³ 22
initial BMP-2 concentration, b_{init}	10^{-12} g/mm ³ 22
threshold nutrient concentration, n_0	2.3×10^{-11} Nm/mm ³ 21
critical nutrient concentration, n_1	9.5×10^{-12} Nm/mm ³ (assumed $N_0/10$)
threshold stem cell density	10^{10} /(g/mm ³) (guess)
reduction factor, α	
FGF-1 reference concentration, g_0	10^{-10} g/mm ³ 22
BMP-2 reference concentration, b_0	10^{-10} g/mm ³ 22
FGF-1 flux coefficient, γ	10^{-2} mm/hr (guess)
BMP-2 flux coefficient, χ	10^{-2} mm/hr (guess)

Table 1. Estimated values of dimensional parameters. In the above, N_C represents number of cells and N_m is number of moles.

We non-dimensionalise the variables as follows:

$$\begin{aligned}x &= x/d, \quad t = t(p_{s_0} C_{total,max_0}/m_{max}), \\(C_S, C_C) &= (C_S, C_C)/C_{total,max_0}, \quad m = m/m_{max}, \\n &= n/N_0, \quad g = g/g_0, \quad b = b/b_0,\end{aligned}\tag{4}$$

The characteristic quantities used to measure the spatial variable, x , cell densities, matrix density and nutrient and growth factor concentrations are the defect thickness, d , the reference maximum total cell density, C_{total,max_0} , the maximum matrix density, m_{max} , the initial nutrient concentration, N_0 and reference growth factor concentrations, g_0 and b_0 , respectively. We choose to measure time, t , based on the matrix production time scale, $m_{max}/(p_{s_0} C_{total,max_0})$. Using the parameter values in Table 1, we estimate this time scale to be approximately 11 days (a unit of time corresponds to approximately 11 days). The dimensionless parameters appearing in the model and their estimate values are provided in Table 2.

For Peer Review

dimensionless parameters	estimated value
stem cell migration (or diffusion) constant, $D_{S_0} = D_{S_0}/(p_{8_0} C_{total,max_0} d^2)$	$10^{-3} - 10^{-2}$
chondrocyte migration (or diffusion) constant, $D_{C_0} = D_{C_0}/(p_{8_0} C_{total,max_0} d^2)$	10^{-3}
nutrient diffusion coefficient, $D_n = D_n m_{max}/(p_{8_0} C_{total,max_0} d^2)$	$(1 - 3) \times 10^2$
matrix diffusion coefficient, $D_m = D_m/(p_{8_0} C_{total,max_0} d^2)$	$10^{-3} - 10^{-2}$
FGF-1 diffusion coefficient, $D_g = D_g m_{max}/(p_{8_0} C_{total,max_0} d^2)$	1.14
BMP-2 diffusion coefficient, $D_b = D_b m_{max}/(p_{8_0} C_{total,max_0} d^2)$	1.14
stem cell proliferation constant, $p_{1_0} = p_{1_0}/(p_{8_0} C_{total,max_0})$	12
stem cell differentiation rate, $p_2 = p_2 m_{max}/(p_{8_0} C_{total,max_0})$	1
stem cell death rate, $p_3 = p_3 m_{max}/(p_{8_0} C_{total,max_0})$	1
chondrocyte proliferation constant, $p_{4_0} = p_{4_0}/(p_{8_0} C_{total,max_0})$	0.012
chondrocyte death rate, $p_5 = p_5 m_{max}/(p_{8_0} C_{total,max_0})$	1
FGF-1 production constant, $p_9 = p_9 m_{max}/(p_{8_0} g_0)$	26.67
FGF-1 degradation rate, $p_{11} = p_{11} m_{max}/(p_{8_0} C_{total,max_0})$	15.4
BMP-2 production constant, $p_{12} = p_{12} m_{max}/(p_{8_0} b_0)$	26.67
BMP-2 degradation rate, $p_{13} = p_{13} m_{max}/(p_{8_0} C_{total,max_0})$	15.4
chondrocyte proliferation rate (from FGF-1), $p_{4_{00}} = p_{4_{00}} m_{max}/(p_{8_0} C_{total,max_0})$	0.012
matrix degradation constant, $p_{8_1} = p_{8_1} m_{max}/p_{8_0}$	1
nutrient uptake constant by stem cells, $p_6 = p_6 m_{max}/(p_{8_0} N_0)$	10^4
nutrient uptake constant by chondrocytes, $p_7 = p_7 m_{max}/(p_{8_0} N_0)$	10^4
FGF-1 matrix deposition rate, $p_{8_{00}}$	0 - 1
threshold nutrient concentration, $n_0 = n_0/N_0$	0.24-0.81
critical nutrient concentration, $n_1 = n_1/N_0$	0.1
threshold stem cell density, $C_{S_{0max}} = C_{S_{0max}}/C_{total,max_0}$	0.35
threshold stem cell density, $C_{S_{0min}} = C_{S_{0min}}/C_{total,max_0}$	0.315
initial stem cell density, $C_S^{(0)} = C_S^{(0)}/C_{total,max_0}$	0.25
initial chondrocyte density, $C_C^{(0)} = C_C^{(0)}/C_{total,max_0}$	10^{-4}
maximum stem cell density, $C_{S,max_0} = C_{S,max_0}/C_{total,max_0}$	0.6
maximum chondrocyte density, $C_{C,max_0} = C_{C,max_0}/C_{total,max_0}$	0.4
matrix density, $m_1 = m_1/m_{max}$	10^{-1}
matrix density, $m_2 = m_2/m_{max}$	10^{-1}
initial matrix density, $m_3 = m_3/m_{max}$	10^{-4}
initial FGF-1 concentration, $g_{init} = g_{init}/g_0$	10^{-2}
initial BMP-2 concentration, $b_{init} = b_{init}/b_0$	10^{-2}
FGF-1 flux coefficient, $\gamma = \gamma/(p_{8_0} C_{total,max_0} d/m_{max})$	1
BMP-2 flux coefficient, $\chi = \chi/(p_{8_0} C_{total,max_0} d/m_{max})$	1
threshold stem cell density reduction factor, $\alpha = \alpha b_0$	100

Table 2. Estimated values of dimensionless parameters.